

Quasielastic neutron scattering study of POSS ligand dynamics

Niina Jalarvo^{1,2,a}, Madhusudan Tyagi^{3,4} and Michael K. Crawford⁵

¹Jülich Centre for Neutron Science, Forschungszentrum Jülich GmbH, 52428 Jülich, Germany

²Chemical and Engineering Materials Division, Spallation Neutron Source, Oak Ridge National Laboratory, Oak Ridge, TN 37861-6475, USA

³NIST Center for Neutron Research, Gaithersburg, MD 20899-8562, USA

⁴Department of Materials Science, University of Maryland, College Park, MD 20742, USA

⁵DuPont Central Research and Development, Wilmington, DE 19880-0400, USA

Abstract. Polyoligosilsesquioxanes are molecules having cage-like structures composed of silicon and oxygen. These molecules can have a wide variety of functional ligands attached to them. Depending on the nature of the ligand, interesting properties and applications are found. In this work we present results from quasielastic neutron scattering measurements of four different POSS molecules that illustrate the presence of strong coupling between the ligand dynamics and the POSS crystal structures.

1. Introduction

Polyoligosilsesquioxanes (POSS) are relatively large (1–2 nm diameter) molecules, that are composed of Si_8O_{12} cages to which a wide variety of possible ligands can be attached (Fig. 1). Depending on the nature of the ligand, interesting properties and application possibilities are found, e.g. selective solubility in solvents, the ability to be dispersed in polymers, the catalytic activity and use as fillers in polymer nanocomposites. Thus, the POSS molecules have attracted much interest recently. Structures of more than 100 POSS molecules have been determined using x-ray diffraction [1], but only a few studies of the dynamical properties of the ligands have been reported [2,3]. We have studied the ligand dynamics of several POSS molecules using quasielastic incoherent neutron scattering (QENS) techniques. In this paper we will compare the ligand dynamics of the 4 different POSS molecules listed in Table 1. These POSS molecules were chosen for this study because, except for M-POSS, they each exhibit interesting structural phase transitions, which are, as we will show in this paper, connected to the ligand dynamics. Therefore, the intermolecular interactions depend upon the POSS ligand dynamics. Study of the POSS ligand dynamics using quasielastic neutron scattering is thus expected to provide insight regarding the intermolecular interactions that lead to structural phase transitions in POSS and other crystals.

2. Experimental

The samples were obtained from Hybrid Plastics and used without further processing. X-ray powder diffraction and NMR were used to confirm the phase purity. QENS data were collected at the backscattering spectrometer BASIS at the Spallation Neutron Source (SNS) [4] and

^a Corresponding author: n.jalarvo@fz-juelich.de

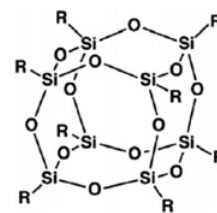


Figure 1. Structure of a POSS molecule. A wide variety of R groups can be attached to the Si-O framework.

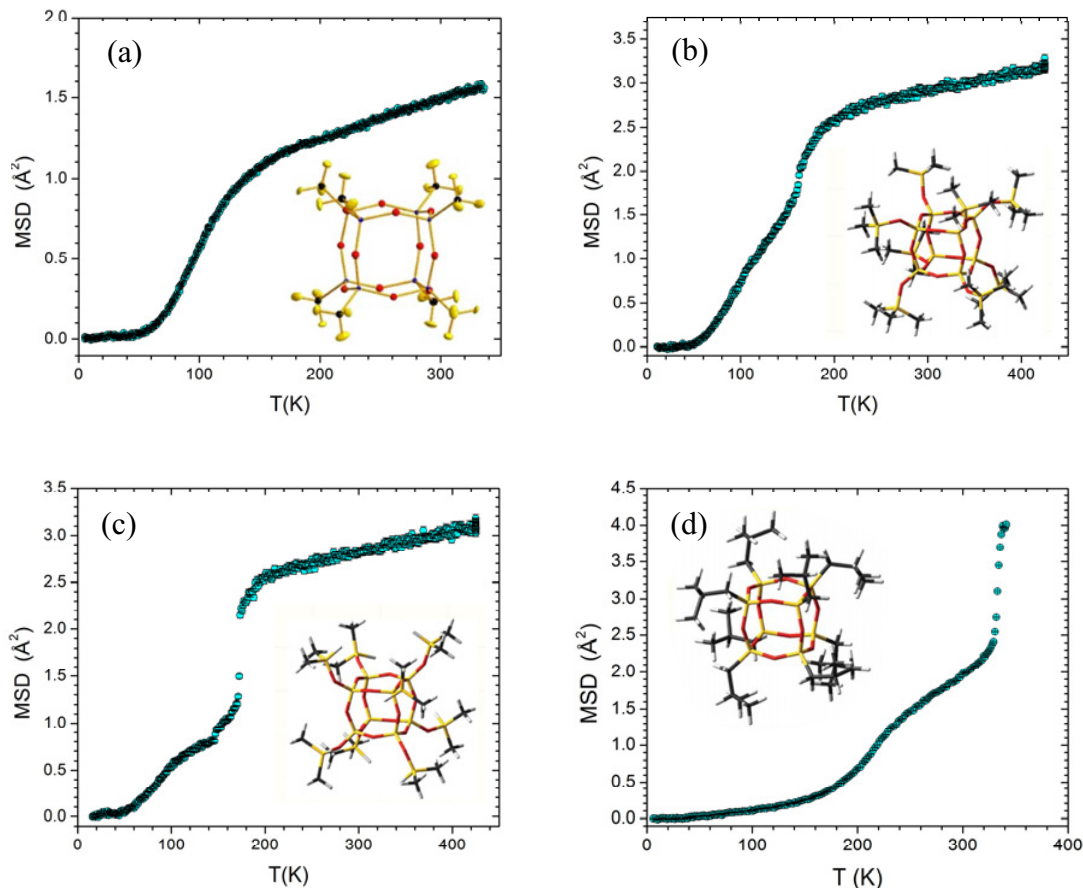
at the high flux backscattering spectrometer (HFBS) at the NIST Center for Neutron Research [5]. The energy resolution at the elastic line (FWHM) was 3.4 and 0.8 μeV and the dynamic range ± 100 and $\pm 17 \mu\text{eV}$ at BASIS and at HFBS, respectively. Cylindrical annular aluminium sample containers were chosen with sample thicknesses giving neutron transmission probability on the order of 90 to 95%. Data sets were collected at temperatures ranging from 4 to 425 K. Low temperature data was used to determine the instrumental resolution function for each sample. In addition data were collected in fixed window mode at HFBS to measure the elastic scattering as a function of temperature.

3. Results and discussion

An overview of the microscopic dynamics as a function of temperature can be obtained from the magnitude of the elastic incoherent neutron scattering (EINS). The EINS reflects exclusively hydrogen dynamics, since all of the other elements in the samples have negligible incoherent neutron scattering cross-sections. The EINS as a function of temperature for each sample was obtained using the HFBS spectrometer by switching the Doppler drive off and using the monochromatic beam of 6.27 Å wavelength. An important quantity derivable from the EINS data

Table 1. The POSS molecules studied in this work, their chemical formulae, the acronyms used and the space groups [1].

Acronym	Molecular name	Chemical formula	Crystal Structure
M-POSS	Octamethyl-POSS	$\text{Si}_8 \text{O}_{12} (\text{CH}_3)_8$	rhombohedral R-3
IBU-POSS	Octaisobutyl-POSS	$\text{Si}_8 \text{O}_{12} (\text{C}_4 \text{H}_9)_8$	monoclinic/triclinic $T < 330 \text{ K}$, rhombohedral $T > 330 \text{ K}$
TMS-POSS	Octatrimethylsiloxy-POSS	$\text{Si}_8 \text{O}_{12} (\text{OSiC}_3 \text{H}_9)_8$	Triclinic P-1 ($T = 295 \text{ K}$)
DMS-POSS	Octadimethylsilane-POSS	$\text{Si}_8 \text{O}_{12} (\text{OSiHC}_2 \text{H}_6)_8$	Rhombohedral R-3 ($T = 200 \text{ K}$)

**Figure 2.** Mean square displacements of (a) M-POSS, (b) TMS-POSS, (c) DMS-POSS and (d) IBU-POSS presented as a function of temperature. Error bars in figures throughout the text represent one standard deviation and if not shown are smaller than the symbols.

is the average mean-square displacement (MSD) of the hydrogen atoms, $\langle \Delta r^2 \rangle$, which can be estimated using the Gaussian approximation

$$I_{el}(Q, T)/I_{el}(Q, T_{min}) = e^{-Q^2 \langle \Delta r^2 \rangle / 3}. \quad (1)$$

Equation (1) was fit to the data, and the resulting MSD values for each sample are illustrated in Fig. 2. This approach assumes that all the hydrogen atoms in the material have the same isotropic MSD, which is not exactly the case for the samples of interest here. Therefore, these values only represent the average MSD for all the hydrogen atoms in each sample.

Figure 2a shows the MSD for M-POSS. At temperatures below 60 K, the MSD follows the expected Debye-Waller type behavior due to harmonic vibrations. Above 60 K the methyl rotations become observable in the measured time scale, and thus the MSD values start to increase rapidly. We have shown in our previous work

[6] that for M-POSS the methyl groups rotate around local 3-fold axes, and this is indeed the only motion that is identified in the QENS spectra. However, the other three samples present much more complex dynamical features over the measured temperature range.

Figure 2b illustrates the obtained MSD values for TMS-POSS. The low temperature MSD features are very similar to those of M-POSS up to about 140 K. This indicates that in TMS-POSS the methyl groups rotate first around their local 3-fold axes, but at temperatures above 140 K different dynamical processes take over. As also observed for M-POSS the rapidly increasing MSD values start to flatten above 140 K, but then there is a second rapid increase of MSD values for TMS-POSS. Near 170 K a discontinuity in the MSD values is observed, suggesting the presence of a first-order structural phase transition. These large MSDs are beyond the values that can be expected for lone methyl group rotations, and most likely the three methyl groups in each ligand start to

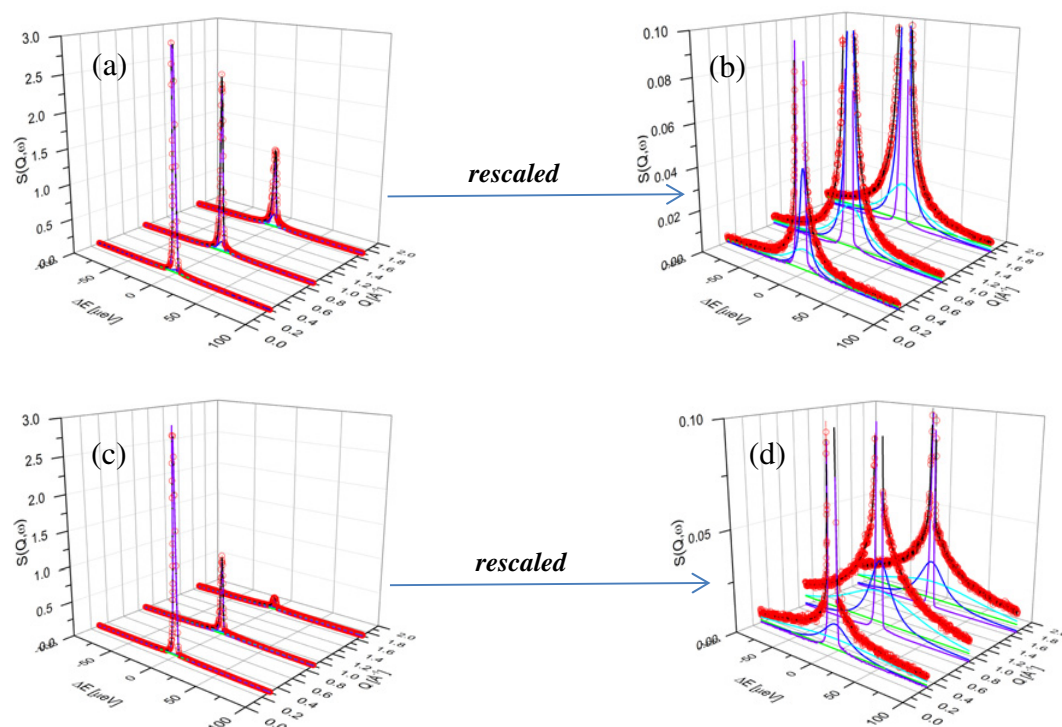


Figure 3. IBU-POSS spectra measured at BASIS (a)&(b) at 270 K, and (c)&(d) at 370 K. The red circles represent the experimental data, and the lines are for the fit function (black), elastic peak (purple), quasielastic terms (blue and turquoise) and background (green).

exchange their locations, i.e. they undergo rotation around the axis passing through the O-Si (siloxy) bond. This type of dynamical transition correlates with a structural transition observed in temperature dependent neutron and X-ray powder diffraction measurements [7].

In Fig. 2c the MSD for the DMS-POSS is shown. Similarities to the M-POSS and to the TMS-POSS can be noted consistent with the fact that the two the methyl groups dominate the hydrogen dynamics of the DMS-POSS ligand. Since the DMS-POSS ligand also has a single hydrogen atom attached to the silane along with the two methyl groups, some differences are also encountered. Whereas the rapid increase for the M-POSS and for the TMS-POSS MSDs starts at around 60 K, this increase is seen for the DMS-POSS at slightly lower temperature. Also the MSD values remain a bit lower, which is a direct reflection of the fact that this averaged MSD includes also the contribution from the single hydrogen. However, up to about 150 K the shape of the MSD curve for DMS-POSS is very similar to that of M-POSS, indicating that the methyl dynamics are similar in these materials, namely rotations around local 3-fold axes. At around 150 and 170 K discontinuities to higher MSD values can be noted. Both of these steps are signs of dynamical transitions in the sample. As for the TMS-POSS, the transition at around 170 K can be assigned to rotation around an axis passing through the O-Si (siloxy) bond, in which, the two methyl groups and the hydrogen atom rotate around this axis. Neutron and synchrotron x-ray powder diffraction data and Raman spectra also indicate structural phase transitions at 145 K and 170 K in DMS-POSS [7].

The IBU-POSS ligand dynamics appear to be very different from those of the three other samples, as can

be noted from the data in Fig. 2d. The MSDs only increase slightly below 180 K, but above this temperature a rapid increase occurs, indicating that observable dynamical processes begin to take place in the sample. This shift of the methyl dynamics to higher temperatures reflects the larger energy barrier to methyl rotation in IBU-POSS, where the methyl groups are attached to carbon atoms, compared to the other three POSS molecules where the methyl groups are instead attached to Si atoms. Another clear dynamical transition in IBU-POSS is observed at about 330 K, which also corresponds to a structural phase transition [2].

Dynamics of these POSS ligands can be observed by QENS measurements. Here we will only discuss the QENS data for the IBU-POSS (Fig. 3). The data for the other samples will be discussed elsewhere [6], [8]. We can clearly note how the elastic intensity decreases as a function of Q , and almost vanishes at higher Q values above the phase transition temperature. The data at these two temperatures obviously require very different dynamical models for their description. To understand the differences in more detail we have fitted the QENS spectra to the following expression:

$$S(Q, \omega) = f \left[p_0 \delta(\omega) + \sum_{i=1}^n p_i \frac{1}{\pi} \frac{\Delta_i(Q)}{\omega^2 + \Delta_i^2} \right] \otimes R(Q, \omega) + B \quad (2)$$

where f is a scaling factor and p_i are the amplitudes of the elastic and quasielastic components. A low temperature data set was used for the instrumental resolution function, $R(Q, \omega)$, which was then convoluted \otimes with the fitted contributions, a δ -function for the elastic contribution and Lorentzian functions with widths Δ_i for the quasielastic

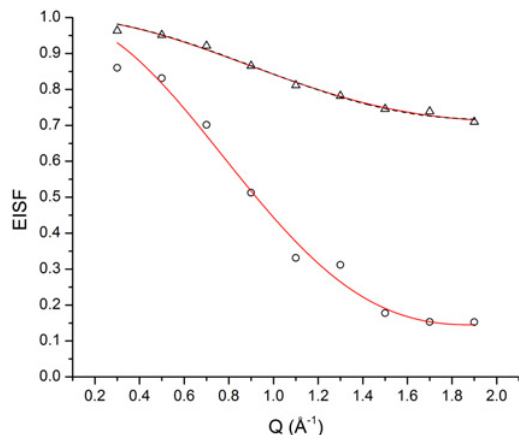


Figure 4. EISF of the broader quasielastic component for IBU-POSS at 270 K (triangles), and at 370 K (circles). The red lines represent fits of continuous rotational diffusion, and the dashed black line represents a fit of 3-site jump diffusion model.

contribution. Each spectrum was fit well by using two Lorentzian functions for the quasielastic part. The widths of the Lorentzian components were Q independent, indicating that the observed processes are localized in nature. Their widths, however, were clearly very different from each other, the broad one being about 3 to 4 times wider in energy than the narrow one. Here we will only discuss the broad component. The elastic incoherent structure factor (EISF) for the broad Lorentzian component is shown in Fig. 4 for 270 and 370 K. Two different models were used to describe the experimental points: a model for jump diffusion among 3 equivalent sites on a circle and a model for continuous rotational diffusion on a sphere. The details of both models are described in literature [9] and can be expressed as follows

$$A_{3\text{ sites}}(Q) = (1 - m) + m \left[\frac{1}{3} + \frac{2}{3} j_0(Qr\sqrt{3}) \right] \quad (3)$$

$$A_{\text{cont}}(Q) = (1 - m) + m[(2l + 1)j^2 l(Qr)]; l = 0, 1, 2, \dots \quad (4)$$

m is the fraction of mobile hydrogen in the material, j_l is the spherical Bessel function of order l , and r is the radius of rotation. Only the first term for the continuous rotational jump diffusion was considered ($l = 0$) and the fit parameters were m and r . At 270 K the fraction of mobile hydrogen is 0.35 ± 0.014 and 0.29 ± 0.13 for the 3-site jump model and for the continuous diffusion model, respectively. This indicates that about 30% of the hydrogen atoms participate in the fast motion. The extracted radii of rotation were $1.33 \pm 0.05 \text{ \AA}$ (3-site jump diffusion) and $1.48 \pm 0.07 \text{ \AA}$ (continuous rotational diffusion), each somewhat higher than the value expected for methyl rotation limited by the methyl C-H bond length (typically around 1 \AA). Considering the fit parameters obtained, neither of these models can describe the methyl dynamics of the IBU-POSS ligands reasonably at 270 K. Therefore we assume that the dynamics also involves other parts of the isobutyl ligand, not only the methyl groups. The data at 370 K cannot be described by the 3-site jump model,

and the continuous rotational diffusion model was used to estimate the fit parameters. It is obvious that at 370 K, a much larger fraction of hydrogen (0.85 ± 0.12) participates in this motion. In addition, the radius of the rotation increases to $1.68 \pm 0.04 \text{ \AA}$. However, a more detailed model is necessary to fully understand the geometry of the isobutyl ligand dynamics. The activation energy for the rotational diffusion characterized by the broad Lorentzian component is 11.4 kJ/mol . This activation energy remains the same below and above the phase transition temperature, but a discontinuity of the quasielastic broadening was observed at the phase transition temperature.

4. Conclusions

A number of dynamic transitions associated with the ligands were observed for TMS-POSS, DMS-POSS and IBU-POSS samples, but not for the M-POSS sample, in the temperature range we explored. The complex ligand dynamics are the driving force for structural phase transitions observed in these samples. Methyl group rotations occur at similar temperatures for the ligands of M-POSS, DMS-POSS and TMS-POSS. However, the onset of methyl rotations is shifted to significantly higher temperatures for the isobutyl ligands of IBU-POSS. This is due to the significantly larger rotational energy barriers for methyl groups attached to carbon atoms compared with silicon atoms.

Neutron research at Spallation Neutron Source was sponsored by the Scientific User Facilities Division, Office of Basic Energy Sciences, U. S. Department of Energy. This work utilized facilities supported in part by the National Science Foundation under Agreement No. DMR-0944772. Identification of commercial products does not imply endorsement by the National Institute of Standards and Technology nor does it imply that these are the best for the purpose. The authors would like to thank K.D. Dobbs (DuPont) for the POSS figures.

References

- [1] D.B. Cordes, P.D. Lickiss, and F.Rataboul, *Chem. Rev.*, **110**, 2081 (2010)
- [2] G. Croce, F. Carniato, M. Milanesio, E. Boccaleri, G. Paul, W. van Beek, L. Marchese. *Phys. Chem. Chem. Phys.*, **11**, 10087 (2009)
- [3] C. Marcolli, P. Lainé, R. Bühler, G. Calzaferri, J. Tomkinson, *J. Phys. Chem. B.*, **101**, 1171 (1997)
- [4] E. Mamontov, K.W. Herwig, *Rev. Sci. Instrum.* **82**, 085109 (2011)
- [5] A. Meyer, R.M. Dimeo, P.M. Gehring, D.A. Neumann, *Rev. Sci. Instrum.*, **74**, 2759 (2003)
- [6] N. Jalarvo, O. Gourdon, G. Ehlers, M. Tyagi, S. K. Kumar, K. D. Dobbs, R. J. Smalley, W. E. Guise, A. Ramirez-Cuesta, C. Wildgruber, M. K. Crawford. *J. Phys. Chem. C.*, **118**, 5579 (2014)
- [7] M. K. Crawford, P. Whitfield, et al. in preparation
- [8] M. K. Crawford, N. Jalarvo, and M. Tyagi et al. in preparation
- [9] Bee, M. *Quasielastic Neutron Scattering*; Adam Hilger: Philadelphia, PA, 1988